The DOI for this manuscript is doi: 10.1175/JAMC-D-12-0300.1

The final published version of this manuscript will replace the preliminary version at the above DOI once it is available.

If you would like to cite this EOR in a separate work, please use the following full citation:

Oludhe, C., S. Arumugam, T. Sinha, N. Devineni, and U. Lall, 2013: The Role of Multimodel Climate Forecasts in Improving Water and Energy Management over the Tana River Basin, Kenya. J. Appl. Meteor. Climatol. doi:10.1175/JAMC-D-12-0300.1, in press.

The Role of Multimodel Climate Forecasts in Improving Water and Energy Management over the Tana River Basin, Kenya

By

C. Oludhe
Department of Meteorology
University of Nairobi, P.O. Box 30197, Nairobi, Kenya
E-mail: coludhe@uonbi.ac.ke

A. Sankarasubramanian*
Department of Civil, Construction and Environmental Engineering
North Carolina State University, Raleigh, NC 27695-7908
E-mail: sankar_arumugam@ncsu.edu

Tushar Sinha
Department of Civil, Construction and Environmental Engineering
North Carolina State University, Raleigh, NC 27695-7908
E-mail: tsinha@ncsu.edu

Naresh Devineni
Columbia Water Center,
Columbia University, New York, NY 10027
E-mail: nd2339@columbia.edu

Upmanu Lall
Columbia Water Center,
Columbia University, New York, NY 10027
E-mail: ula2@columbia.edu

*** - Contact Author**

(Under Review in the Journal of Applied Meteorology and Climatology)

Abstract

The Masinga Reservoir located in the upper Tana River Basin, Kenya, is extremely important in supplying country's hydropower and protecting downstream ecology. The Dam serves as the primary storage reservoir, controlling streamflow through a series of downstream hydro-electric reservoirs. The Masinga dam's operation is crucial in meeting the power demands thus contributing significantly to the country's economy. La Nina related prolonged droughts of 1999-2001 resulted in severe power shortages in Kenya. Therefore, seasonal streamflow forecasts contingent on climate information are essential to estimate pre-season water allocation. Here, we utilize reservoir inflow forecasts downscaled from monthly updated precipitation forecasts from ECHAM4.5 forced with constructed analogue SSTs and multimodel precipitation forecasts developed from ENSEMBLES project to improve water allocation during April-June (AMJ) and October-December (OND) seasons for the Masinga reservoir. Three-month ahead inflow forecasts developed from ECHAM4.5, multiple GCMs and climatological ensemble are ingested into a reservoir model to allocate water for power generation by ensuring climatological probability of meeting the end of the season target storage required to meet seasonal water demands. Retrospective reservoir analysis shows that inflow forecasts developed from single GCM and multiple GCMs perform better than climatology by reducing the spill and increasing the allocation for hydropower during above-normal inflow years. Similarly, during below-normal inflow years, both these forecasts could be effectively utilized to meet the end of the season target storage by restricting releases for power generation. The multimodel forecasts preserves the end of the season target storage better than the single model inflow forecasts by reducing uncertainty and the overconfidence of individual model forecasts.

1.0 Introduction

Recent studies focusing on the teleconnection between Sea Surface Temperature (SST) conditions and regional/continental hydroclimatology show that interannual and interdecadal variability in exogenous climatic indices modulate both global and regional scale rainfall (Ropelewski and Halpert, 1987) and streamflow patterns (*e.g.*,Dettinger and Diaz, 2000; Piechota and Dracup, 1996). Advancement in understanding the linkages between exogenous climatic conditions such as tropical SST anomalies to local/regional hydroclimatology offer the scope of predicting season ahead and long-lead time (12 to 18 months) streamflow (Maurer and Lettenmaier, 2003; Souza and Lall, 2003). Considerable improvement in the skill of seasonal climate forecasts over the last decade has also been achieved using the slowly evolving boundary conditions such as SSTs in the tropical oceans (Goddard et al. 2003). Seasonal forecasts of streamflow could also be utilized effectively for multipurpose water allocation and to prepare adequate contingency measures to mitigate hydroclimatic disasters (Voisin et al. 2006; Georgakakos and Graham, 2008; Golembesky et al. 2009). Hence, the application of climate based information for water management has been shown to result in improved benefits over the long term in comparison to the benefits that would be obtainable under no-forecasts (climatology) based operation. Still, application of climate forecasts for improving water management faces various challenges partly due to the uncertainty in climate forecasts (Pagano et al. 2001; Pagano et al. 2002) as well as due to the challenges in translating probabilistic forecasts for operational guidance (Sankarasubramanian et al. 2009).

Recent studies on operational streamflow forecasts development show that seasonal streamflow forecasts downscaled from monthly updated climate forecasts are quite effective in reducing the uncertainty in intra-seasonal water allocation (Sankarasubramanian et al. 2008;

Sankarasubramanian et al. 2009). Efforts to reduce uncertainty in climate forecasts have also focused on combining climate forecasts from multiple climate models (Rajagopalan et al. 2002; Devineni and Sankarasubramanian, 2010a, 2010b). Recent studies based on multimodel combination approach indicate better streamflow forecasting skill than any individual forecast model as the skill of the multimodel ensembles is maximized by assigning optimal weights to each GCM (Robertson et al. 2004; Devineni et al. 2010a, 2010b). Studies have also shown the utility of multimodel streamflow forecasts derived from low-dimensional models in invoking restrictions and water conservation measures during drought years (Golembesky et al. 2009). Low dimensional models primarily employ the dominant modes of variability in the predictors (e.g., precipitation forecasts from GCMs) to explain the variability in the predictand (e.g., precipitation/streamflow). For instance, Golembesky et al. (2009) utilized probabilistic multimodel streamflow forecasts to invoke water-use restrictions for improving the operation of Falls Lake reservoir, Neuse basin during below normal inflow years. One important usefulness of multimodel climate forecasts is in reducing the overconfidence of individual models resulting in lesser false alarms and missed targets (Devineni and Sankarasubramanian, 2010a; Weigel et al. 2008). This has important implications since multimodel climate forecasts can increase the confidence of stakeholders towards application of climate information for water management.

The main intent of this study is to evaluate the performance of probabilistic streamflow forecasts developed from single General Circulation Model (GCM) and from multimodel climate forecasts in improving the hydropower generation for the Tana River basin, Kenya. Tana River basin accounts for about 57% of the total hydropower generated in Kenya and our analysis is focused on the Masinga Reservoir system, which accounts for about 67% of the total storage capacity in the Tana River basin. For developing the reservoir inflow forecasts, the study utilizes

3-month ahead precipitation forecasts from ECHAM4.5 General Circulation Model (GCM) forced with constructed analogue SST forecasts and the multimodel climate forecasts developed from the study of Devineni and Sankarasubramanian (2010a). The reservoir management model adopted here is a simplified version of the dynamic allocation framework reported by Sankarasubramanian et al. (2009).

The manuscript is organized as follows: Section 2 provides baseline information on the Tana River basin and its linkage to El-Nino Southern Oscillation (ENSO) along with the seasonal streamflow forecasts developed from ECHAM4.5 and from multimodel climate forecasts. Following that, we present a brief description of the Masinga reservoir simulation model and the retrospective reservoir analyses design. Section 4 compares the utility of streamflow forecasts derived from ECHAM4.5 and multiple climate models with climatology in improving the hydropower generation from the Masinga reservoir. Finally, in Section 5, we summarize the findings of the study and also give conclusions.

2.0 Hydroclimatology of the Tana basin and Streamflow Forecasts Development

Kenya experienced major extreme climatic events in the recent past such as El-Niño related floods in 1997/1998 and 2009/2010 and La Niña related droughts in 1999/2000 and 2008/2009, which led to severe socio-economic impacts in the country. Specifically, inadequate rainfall during the prolonged 1999-2000 drought led to severe water scarcity and shortage in electrical power supply causing serious power rationing throughout the country. In particular, the estimated losses in hydropower generation and industrial production due to water shortage during the 1999/2000 drought were over 2 billion US dollars (Mongaka et al., 2006). Such enormous losses related to the extreme events underscores the need to translate the climate based streamflow forecasts information into planning, risk management and decision-making to minimize socio-economic impacts and to meet increased energy demands in the near future.

Kenya is highly dependent on hydropower which constitutes over 75% of the total electricity generated in the country. The bulk of this electricity is obtained from five generating plants along the Upper Tana River Basin (Figure 1a), namely Masinga (40 MW), Kamburu (94.2 MW), Kindaruma (44 MW), Gitaru (225 MW) and Kiambere (156 MW), typically known as the Seven-Forks Dams (See Figure 1a). Kenya Electricity Generating Company Limited (KenGen) is the leading electric power generation company in Kenya producing about 80 percent of electricity from hydropower. The Masinga Dam, the uppermost reservoir, controls the flow of water through a series of downstream hydro-electric reservoirs. The Masinga catchment area lies between 0°7′–1°15′S and 36°33′–37°46′E and has an area of about 7,354 km^2. The reservoir has a capacity of 1,560 million m^3 at Full Supply Level (FSL) with a surface area 120 km^2. The spillway for Masinga dam is 1,056.5 meters above mean sea level which corresponds to the FSL. The minimum operating level is 1,035.0 meters above mean sea level. Tana River basin experiences bimodal precipitation pattern and accordingly dominant runoff seasons occur during April – Mary–June (AMJ) and October – November – December (OND). Observed inflows at the Masinga Dam are available from 1940 to till date. Inflows during AMJ, which are heavily influenced by SST variations in the Indian Ocean (Mutai and Ward, 2000), contribute more than 46% of the total annual inflows into the dam (Figure 1b). Inflows during the OND season account for 26% of the annual flows and its interannual variations are significantly associated with ENSO variations (Mutai and Ward, 2000). The correlation between OND flows and JAS (July-August-September) Nino3.4, a commonly used index denoting ENSO conditions which indicate the average SSTs over 170 W-120W and 5S-5N, over the 1947-2005 period is 0.42. This strong association between SST and inflows indicates the potential in linking climate forecasts for developing season-ahead inflow forecasts for the Tana River basin.

Seasonal streamflow forecasts based on exogenous climate indices can be obtained using both dynamical and statistical modeling approaches. The dynamical modeling involves coupling of a hydrological model with a Regional Climate Model (RCM) that preserves the boundary conditions specified by the General Circulation Models (GCM) by considering the topography of a region (e.g., Leung et al., 1999; Nijssen et al., 2001). However, uncertainty propagation from the coupling of these models (Kyriakidis et al. 2001) and converting the gridded streamflow/precipitation forecasts into reservoir inflow forecasts pose serious challenges in employing dynamical downscaling for water management applications. On the other hand, statistical modeling basically employs statistical models to downscale GCM outputs to develop streamflow forecasts at a desired location (Gangophadhyay et al., 2005). Studies have also related well-known climatic modes to observed streamflow in a given location using a variety of statistical models ranging from simple regression (e.g., Hamlet and Lettenmaier, 1999) to complex methods such as linear discriminant analysis (Piechota et al., 2001), spatial pattern analysis (Sicard et al., 2002), and semi-parametric resampling strategies (Souza and Lall, 2003). Although both approaches have their advantages and limitations, statistical modeling approach is the least data intensive and is very relevant in regions such as Kenya, where high resolution spatial data to run regional climate and hydrologic models are not readily available.

2.1 Multimodel Inflow Forecasts Development using Multimodel Climate Forecasts

The primary intent of this paper is to utilize inflow forecasts developed using multimodel climate forecasts and compare their performance with inflow forecasts developed using single GCMs and with climatological inflows. Recent studies on reducing the uncertainty of climate forecasts shows that combining multiple models result in reduced false alarms and missed targets resulting in improved probabilistic climate forecasts (Rajagopalan et al., 2002; Devineni and Sankarasubramanian, 2010b). In this study, we utilize the multimodel precipitation forecasts developed by Devineni and Sankarasubramanian (2010b) for developing multimodel inflow forecasts for the Masinga reservoir. The multimodel precipitation forecasts for the AMJ and OND seasons are developed by combining five coupled GCMs (CGCMs) and climatology (i.e. observed precipitation) based on the methodology described in Devineni and Sankarasubramaniam (2010b). The precipitation forecasts from multiple models along with the climatology are combined by analyzing the skill of the candidate models contingent on the Nino3.4 state. The main advantage of combining multiple GCMs conditional on the predictors' state is that the approach assigns higher weights for climatology and lower weights for the CGCMs particularly if the skill of a candidate model is poor under ENSO conditions. For additional details and a complete discussion on the multimodel combination methodology, see Devineni and Sankarasubramaniam (2010a, 2010b).

Retrospective precipitation forecasts from the European Union's ENSEMBLES project (Weisheimer et al. 2009) were used to develop the multimodel forecasts over the Masinga River Basin. Table 1 provides details on the five CGCMs considered in the ENSEMBLES experiment for developing multimodel precipitation forecasts. Seven-month ahead retrospective climate forecasts were developed on 1st February, 1st May, 1st August and 1st November for the period 1960-2005 using the respective months' initial conditions. For this study, we considered CGCMs' SST forecasts and precipitation forecasts issued on 1st February (1st August) to develop multimodel precipitation forecasts. For instance, monthly precipitation forecasts issued in 1st February (1st August) for the period AMJ (OND) are converted into tercile forecasts for each

CGCM and the tercile forecasts are combined based on the Devineni and Sankarasubramanian (2008) algorithm to develop the multimodel tercile forecasts. Given the tercile probabilities, $PF_t^{i,j}$, with '*i*' (1= below-normal, 2=normal and 3= above normal) denoting the tercile categories, '*j*' (1= AMJ and 2= OND) indicating the season and '*t*' denoting the year of forecast over the period 1960-2005, we estimated the conditional mean, μ_j^t, and conditional variance, σ_j^t, of the forecast using equations (1) and (2) by assuming the conditional distribution as normal. Given climatological 33rd and 67th percentiles, $P^{0.33,\,j}$ and $P^{0.67,\,j}$, for a given season, we used the tercile probabilities issued for a given season in a particular year to estimate the condition mean and variance by solving the simultaneous equations in (1) and (2).

$$\frac{P^{0.33,j} - \mu_t^j}{\sigma_t^j} = z_t^{1,j} \qquad (1)$$

$$\frac{P^{0.67,j} - \mu_t^j}{\sigma_t^j} = z_t^{2,j} \qquad (2)$$

The standard normal variates, $z_t^{1,j}$ and $z_t^{2,j}$, are obtained based on the inverse of the cumulative distribution function of the standard normal distribution with the respective cumulative probabilities, $CF_t^{1,j} = PF_t^{1,j}$ and $CF_t^{2,j} = PF_t^{1,j} + PF_t^{2,j}$, being computed based on the tercile precipitation forecasts. Once we obtain the conditional mean, μ_j^t, and conditional variance, σ_j^t, we can generate realizations from the normal distribution. The conditional mean of the multimodel forecast over the Masinga catchment area over four grid points (Figure 1a) and the previous month streamflow, Q_{t-1}, were used as predictors in the principal component regression to develop the inflow forecasts for the Masinga Dam. We capture the role of initial land surface conditions by using the previous month streamflow as a predictor in developing streamflow forecasts. Filled stars in Figure 1a indicate the selected grid points of multimodel precipitation forecasts and open stars indicate the selected grid points of precipitation forecasts from the ECHAM4.5 GCM. We considered principal components regression, since the forecasts from these four grid points were correlated. All the GCMs from ENSEMBLES experiment and ECHAM4.5 atmospheric GCM were almost at the same resolution. Our previous study combined the individual CGCMs precipitation forecasts to develop multimodel precipitation forecasts.

To compare the performance of multimodel climate forecasts, we also consider precipitation forecasts from a single GCM – ECHAM4.5 forced with constructed analogue SSTs. Retrospective precipitation forecasts from ECHAM4.5 are available at IRI for 7 months in advance for every month beginning January1957 with a resolution of 2.8°X2.8° (http://iridl.ldeo.columbia.edu/SOURCES/.IRI/.FD/.ECHAM4p5/.Forecast/ca_sst/.ensemble24/.MONTHLY/.prec/). To force the ECHAM4.5 with SST forecasts, retrospective monthly SST forecasts were developed based on the observed SST conditions in that month based on the constructed analogue approach. For additional details on ECHAM4.5 precipitation forecasts, see Li and Goddard (2005) (http://iri.columbia.edu/outreach/publication/report/05-02/report05-02.pdf). The ensemble mean which is computed from 24 realizations of ECHAM4.5 precipitation forecasts obtained based on different initial conditions was downloaded over the Masinga catchment area from IRI data library for the period 1957-2005. We utilize the ensemble mean of precipitation forecasts issued at the beginning of two rainy seasons (April – May – June (AMJ) and October – November – December (OND)), April 1^{st} and October 1^{st}, along with the previous month streamflow (March/September) as additional predictor. Though this result in comparison of precipitation forecasts from multimodels and ECHAM4.5 at two different lead times, from the perspective of water management, the allocation decisions are usually done at the beginning of the season. Thus, in the context of application, the best single model forecast available at the beginning of the season is used.

Principal Components Regression (PCR): Since the gridded precipitation forecasts over a given region are spatially correlated, employing precipitation forecasts from multiple grid points as predictors would raise multicollinearity issues in developing the regression. PCR, which is a commonly employed approach in Model Output Statistics (MOS) (Wilks, 1995), eliminates systematic errors and biases in GCM fields and also recalibrates the principal components (PCs) of GCM fields to predict the hydroclimatic variable of interest using regression analyses. In this context, the predictand is the streamflow (Q_t) over the season (AMJ/OND) and the predictors are the previous month streamflow (Q_{t-1}) and the ensemble mean of precipitation forecasts from ECHAM4.5 GCM or the multimodel ensemble mean obtained using equations (1) and (2). Using the principal components of the predictors, we developed regression relationship based on equation (2):

$$ln(Q_t) = \hat{\beta}_0 + \sum_{k=1}^{K} \hat{\beta}_j * PC_t^k + \hat{\varepsilon}_t \qquad (3)$$

where Q_t denotes the observed streamflow during the AMJ/OND season in year 't', PC_t^k denotes the 'k'th PCs from the retained 'K' PCs of precipitation forecasts and $\hat{\beta}$s denote the regression coefficients whose estimates are obtained by minimizing the sum of squares of error. We employed step-wise regression to select 'K' PCs out of the rotated grid points of precipitation for developing the PCR model.

Using principal components regression (PCR), we developed single model (SM) inflow forecasts and multimodel (MM) inflow forecasts to obtain the leave-one-out cross-validated mean seasonal (conditional mean) streamflow forecasts for the AMJ (OND) season. Using the point forecast error obtained from the PCR, we obtained the conditional variance of the seasonal streamflows to develop the probabilistic reservoir inflow forecasts. Residual analyses of the PCR based on the quantile plots and skewness test on the residuals showed that the normality assumption is valid. This indicates that the seasonal flows during the AMJ and OND season could be assumed as a log-normal distribution. Based on this assumption, we developed 500 ensembles of the seasonal streamflows in log-space using the conditional mean and the point forecast error obtained from the PCR. These ensembles are eventually transformed back to the original space for developing the probabilistic inflow forecasts that could be forced with the Masinga reservoir model.

Figure 2a (2b) show the conditional mean of the SM and MM seasonal streamflow forecasts for the period 1991 – 2005 developed based on the ECHAM4.5 and multimodel precipitation forecasts for the AMJ (OND) seasons. All the forecasts for the single model (multimodel) in Figure 2 are obtained in a leave-one-out cross-validated mode using the observed flows and the predictors for the period 1961-2005 (1961 – 2005). Since the multimodel climate forecasts from ENSEMBLES project are available only up to 2005, we have evaluated the skill of the multimodel inflow forecasts only up to 2005. The inset in Figure 2 shows the verification statistics for the multimodel (single model) inflow forecasts based on correlation coefficient and root mean square error computed between the ensemble mean of the forecasted streamflow and the observed streamflow over the period 1961-2005 (1961-2005). From Figure 2, we observe that the multimodel streamflow forecasts slightly perform better than the single model forecasts in predicting the conditional mean. It is important to note that the single model inflow forecasts for the AMJ and OND seasons were developed using 3-month ahead ECHAM4.5 precipitation forecasts issued at the beginning of April and October respectively. On the other hand, the multimodel precipitation forecasts issued at the beginning of 1st February and 1st August were employed in developing the AMJ and OND inflow forecasts, which results in a lead time of two months for both seasons. We ingest these leave-one-out cross-validated probabilistic streamflow forecasts available to the probabilistic reservoir simulation model over the period 1991 – 2005 for evaluating the utility of streamflow forecasts developed from single model and multimodel precipitation forecasts in improving the water and energy management for the Masinga Reservoir.

3.0 Masinga Reservoir Simulation Model

The reservoir simulation model used here is a simplified version of the detailed dynamic water allocation framework presented in Sankarasubramaniam et al. (2009). Given seasonal (*T*-month lead) streamflow forecasts (as ensembles) q_t^k and initial reservoir storage, S_{t-1}, at the beginning of the allocation period, the reservoir simulation model determines the seasonal release R_t^h *and* R_t^w for hydropower generation and city of Nairobi water supply respectively. Here, t =1, 2, . . . , N denotes the forecast years (N=total number of years of retrospective forecasts; 1991-2005 for multimodel forecasts and 1991-2005 for ECHAM4.5 downscaling), and k =1, 2,..., K index represents a particular realization within the ensemble. In addition, the water allocation model incorporates an end of the season target storage, S_T^* (T denoting the forecast lead time in months) that is associated with a failure probability p_s. For instance, in the case of Masinga reservoir S_T^* corresponds to the target storage of 1572 MCM (1560 MCM) at the end of June (December) for meeting the demand during the months with low rainfall. Figure 3a shows the operational rule curves for the Masinga Dam. Using the basic continuity equation, the seasonal storage equations for each ensemble member k are updated for the forecasting year t

$$S_{T,t}^{k} = S_{t-1,k} + q_t^k - E_t^k - R_t^h - R_t^{ws} - SP_{k,t} \qquad \ldots (4)$$

where seasonal storage equations are constrained so that the storage is between the minimum and maximum possible storage, $S_{\min}$ and $S_{\max}$, respectively

$$S_{T,t}^{k} = \min(S_{T,t}^{k}, S_{\max}), \qquad S_{T,t}^{k} = \max(S_{T,t}^{k}, S_{\min}) \qquad \ldots (5)$$

$SP_{k,t}$ is the spill which occurs if $S_{T,t}^{k}$ > $S_{\max}$, and could be obtained based on the constraints from equations (4) and (5). The release for hydropower R_t^{hydro} is converted into net hydropower HP_t generated from the turbines based on the elevation storage relationship of the reservoir. Evaporation, E_t^k is also computed as a function of average storage during the season using the water spread area and storage information of the reservoir specified in equation (6).

$$E_t^k = \psi_t \delta_1 ((S_{t-1,k} + S_{T,k}^{k})/2)^{\delta_2} \qquad \ldots (6)$$

where ψ_t = seasonal evaporation rate and δ_1 and δ_2 = coefficients describing the area–storage relationship. We employed spline interpolation technique for obtaining the water spread area corresponding to the average season storage computed for each ensemble. It is important to note that the evaporation is evaluated implicitly for each realization in the ensemble. The estimated average evaporation rate (ψ_j) = 0.402 mm and 0.502 mm for the AMJ and OND seasons respectively.

The objective is to determine R_t^h, such that the probability of having the end of the season storage, $S_{T,t}$, less than the target storage, S_T^*, is small which is represented by its failure probability (Prob), p_s, using

$$\text{Prob}(S_T \le S_T^*) \le p_s \qquad \ldots (7)$$

Given the water supply release is very small (35 MCM) compared to the hydropower release, we considered climatological probability for p_s (= 0.5) which implies that the target storage could be violated 50% of the time under the retrospective forecast-based analysis. Reducing p_s will result in reduced releases for hydropower resulting in increased spill from the reservoir.

Prior to performing the retrospective reservoir analyses using the streamflow forecasts, we performed model verification from 1991 to 2005 by comparing the reservoir model's ability to simulate the observed end of June storages. The simulations were performed by forcing the model with the observed flows during AMJ and initial storages in April to determine the end of the June storages by allocating the reported releases for water hydropower generation. Figure 3b shows the observed and model predicted stages at the end of June—the end of the season stage. The observed and modeled storages obtained from the reservoir model were converted into stages using the available stage–storage relationship for the Masinga Reservoir. From Figure 3b, we understand that the developed model is quite reasonable in predicting the observed June storages upon simulation with observed flows and the reported hydropower and water supply releases. This gives the confidence in employing the simulation model presented here for further analyses that utilize the seasonal streamflow forecasts from two models for improving water and energy management.

In this study, we consider three inflow forecasting schemes (a) streamflow developed using ECHAM4.5 precipitation forecasts, (b) multimodel precipitation forecasts obtained by combining five GCMs from the ENSEMBLES project and (c) climatological ensemble. Each scheme provides 500 members/realizations for a given season indicating the conditional distribution of the inflows into the Masinga Dam. The climatological ensemble for each season is obtained by leaving out the particular year's observation from the observed inflow (1940-2005) with the remaining 70 years having equal chances of getting selected in the ensemble. This is reasonable, since the lag-1 correlation on the seasonal flows is almost zero. For each of the forecasting schemes, we first obtain the p_s. Based on the end of the season target storage probabilities estimated from climatological forecasts (accepted climatological risks), we explore the possibilities of modifying the releases from current releases to increase the power generated during above normal storage conditions and impose restrictions during below normal storage conditions. For instance, if the climate-information based forecasts (i.e., schemes (a) and (b)) suggests lower (higher) probability of $S_T \leq S_T^*$ is lesser than 0.5, then we increase (decrease) the releases such that p_s =0.5. Thus, we obtain revised releases for the single model and multimodel inflow forecasts as well as for the climatological ensemble by ensuring p_s = 0.5 for each year during 1991-2005. Using the revised releases for each of the three forecasting schemes, we run the reservoir model with the observed inflows to obtain the end of the season target storages. The basis for comparing the performance of the three forecasting schemes is based on the end of the season target storages, spill and generated hydropower by combining the releases that ensures p_s=0.5 under the three forecasting schemes with the observed inflows for the period 1991-2005. This retrospective analysis similar to our previous studies (Golembesky et al., 2009; Sankarasubramanian et al., 2009) provides us an understanding on what would have happened if the candidate inflow forecasts were applied over the period 1991-2005.

4.0 Results and Analysis

This section presents the retrospective analyses for understanding the utility of single model and multimodel inflow forecasts in improving the hydropower generation for the Masinga Dam utilizing the three candidate forecasting schemes. Since the multimodel forecasts are available only up to 2005, all the results presented in this section consider the period 1991-2005 for multimodel forecasts, whereas results for single model forecasts and climatological ensemble are presented for the period 1991-2005.

4.1 End of the Season Target Storage Probabilities

To begin with, we first evaluate the ability of the three candidate forecasting schemes in estimating the probability of meeting the June and December storage for the reported seasonal releases from Masinga over the period 1991-2005 without constraining the releases being p_s=0.5. Given that most of the reservoirs can hold water for more than the seasonal demand, the entire demand could be met with 100% reliability. However, we can modify the reservoir releases by comparing the ability of the three forecasting schemes in estimating probability of meeting the end of the season target storage (Prob$(S_T < S_T^*)$).

Figure 4 shows the estimates of Prob$(S_T < S_T^*)$ for the three forecasting schemes where S_T^*=1560 MCM and S_T^*=1572 MCM for AMJ (Figure 4a) and OND (Figure 4b) seasons respectively. The probability estimates shown were obtained from each streamflow forecasting model and from climatological ensembles. Figure 4 also shows the observed streamflows (Q_t)in each year suggesting their tercile category (Q_t < 0.33 percentile – Below-Normal (Obs_BN); Q_t < 0.66 percentile — Above-normal (Obs_AN); otherwise — Normal (Obs)). Both Figures 4(a) (AMJ releases) and Figure 4(b) (OND releases) demonstrate that the estimates of Prob$(S_T < S_T^*)$ vary depending on the forecasted streamflow potential by each model. Since all the three inflow forecasts were run with the same initial conditions recorded at the beginning of the season in the Masinga Dam, any difference in estimating the Prob$(S_T < S_T^*)$ among the forecasts should be primarily due to the skill of the inflow forecasts.

Figures 4a and 4b show clearly that the estimates of $\mathrm{Prob}(S_T < S_T^*)$ from streamflow forecasts are above (lower) the estimates of $\mathrm{Prob}(S_T < S_T^*)$ from climatological ensembles during below-normal (above-normal) inflow conditions, which indicates the skill of the inflow forecasts in predicting the observed inflows during the AMJ and OND seasons. This is expected as the probability of attaining the end of the season target storage will be low (high) during below-normal (above-normal) inflow conditions. We also observe that the estimates of $\mathrm{Prob}(S_T < S_T^*)$ in Figures 4a and 4b differ for each streamflow forecast, as each forecasts exhibit different skill. During normal years (empty circles on the secondary Y axis), the difference between the estimates of $\mathrm{Prob}(S_T < S_T^*)$ is very small indicating all the inflow forecasts from three schemes contain similar probabilistic information in predicting the season-ahead inflows. The only exceptions are during AMJ 1995 and AMJ 1997 under which the multimodel forecasts estimate $\mathrm{Prob}(S_T < S_T^*)$ are very different from that of ECHAM4.5 based inflow forecasts and climatological ensemble.

Comparing the performance of multimodel inflow forecasts with inflow forecasts developed using ECHAM4.5 precipitation forecasts, we infer that multimodel forecasts forecasts perform more consistently in indicating below-normal inflow storage conditions. For instance, multimodel forecasts correctly estimate the $\mathrm{Prob}(S_T < S_T^*)$ in comparison to the climatological estimates of $\mathrm{Prob}(S_T < S_T^*)$ in year 1993, 1996 for the AMJ season and in year 2001 for the OND season in predicting the below-normal inflow season. Further, $\mathrm{Prob}(S_T < S_T^*)$ estimated using single model inflow forecasts are shown to be significantly higher (Figure 4) than that of multimodel estimate of $\mathrm{Prob}(S_T < S_T^*)$ during above-normal and below-normal conditions. This is primarily due to the overconfidence of single model in predicting below-normal and above-normal conditions as reported by previous studies (Weigel et al., 2008; Devineni and Sankarasubramanian, 2010a). On the other hand, estimates of $\text{Prob}(S_T < S_T^*)$ from multimodel forecasts are much closer to the climatological estimates of $\text{Prob}(S_T < S_T^*)$ since multimodel forecasts reduce the overconfidence of individual models resulting in reduced false alarms. Both multimodel and single model forecasts incorrectly estimate $\text{Prob}(S_T < S_T^*)$ for AMJ 2003 – an above-normal inflow season – with the model-based target storage probabilities being higher than climatological counterpart. In general, having inflow forecasts from multiple models provides more confidence in developing appropriate scenarios for application. We present in the next section a more detailed comparison on the performance of ECHAM4.5-based inflow forecasts and multimodel in improving the energy management.

4.2 Hydropower generation for Masinga Reservoir utilizing Multimodel forecasts

Though results showed in Figure 4 did not ensure p_s = 0.5 for each forecasting scheme, the estimates of $\text{Prob}(S_T < S_T^*)$ obtained from the three models show their ability to change according to the nature of inflow conditions. For the next set of analysis, we ensure p_s = 0.5 such that releases from the reservoir could be adjusted so that the desired end of the season target storage probability is maintained. The basis behind this analysis is that the user accepts risk of meeting the target storage based on climatological inflows derived using observed inflows. The idea is that releases (Figure 5) are adjusted by ensuring the ps = 0.5 for both forecasted and climatological inflows and then those releases are validated by estimating the actual hydropower generation (Figure 6), spill (Figure 7) and the end of the season storage (Figure 8) that could have occurred based on the the actual inflows during the season.

Given that p_s = 0.5 for each season in a given year, we utilize the three forecasting schemes to modify the reservoir releases to increase (reduce) hydropower generation if the inflow forecasts suggest above normal (below normal) conditions. For instance in AMJ 1998 (above normal inflow year), in Figure 4, estimates of $\text{Prob}(S_T < S_T^*)$ are almost zero for both single model and multimodel forecasts indicating that the probability of attaining the target storage is very high. Hence, given that the accepted risk in meeting the target storage (p_s) is 0.5, one can increase the water releases (determined from the reservoir simulation model) for hydropower generation to meet the target storage constraint. Similarly, during AMJ 2000 (below normal inflow year), since both forecast models suggest that the probability of meeting the target storage is very low, we can enforce restrictions on the releases for hydropower to ensure p_s =0.5. Such information on reduced potential of generating hydropower could be utilized for increasing the firm power generation from other systems.

The main intent of this study is to understand the utility of multimodel streamflow forecasts in improving the water allocation for hydropower generation. For this purpose, the AMJ /OND multimodel inflow forecasts are utilized to modify the releases for hydropower generation over the three month period in the season during 1991-2005 by enforcing the end of the season storage constraint to be equal to 0.5. We used the observed storage on March 31 (September 30) of each year during 1991 – 2005 as the initial storage (S_{t-1}) for AMJ (OND) season. By combining the streamflow forecasts,(q_{tk}), issued in March (September) with the observed storage at the end of March (September), we obtain releases for hydropower use, $R^h{}_t$, by constraining p_s = 0.5 in equation (7). The revised releases that constraints p_s= 0.5 are combined with the observed inflows to infer what could have happened on the generated hydropower and in meeting the target storage if the forecast-suggested inflows were used as the allocation policy for the season.

Figure 5 shows the estimated difference in the releases obtained using climatological ensemble (forecasting scheme c) to the releases suggested by the single model and multimodel forecasts for improving hydropower generation for AMJ (Figure 5a) and OND (Figure 5b) seasons over the period 1991 – 2005. The releases for all the three forecasting schemes are obtained by ensuring p_s= 0.5. The figure also shows the actual observed inflow during the period as below normal, normal or above normal condition on the secondary Y-axis. A positive (negative) change indicates that the model suggests higher probability of not meeting the target storage resulting in reduced (increased) release from the climatological ensembles predicted releases. From figure 5, we observe that single model and multimodel forecasts suggest an increase (decrease) in releases compared to during above normal (below normal) inflow years. Further, we can also see that the multimodel forecasts suggest more water release during above normal years compared to single model forecasts. Similarly, during below normal years, the multimodel forecasts suggest more reduction in release from the actual observed release compared to SM forecasts.

Given that the Masinga reservoir is primarily operated for hydropower generation, we also estimated the amount of hydropower (in GWH) that results each year from operating the reservoir based on the seasonal forecasts. In other words, we combine the model determined releases with observed inflows to simulate to actual amount of hydropower that is generated based on the storage – elevation relationship of the reservoir. Figure 6 shows the estimated change in generated hydropower from the reservoir from both the forecasts. Analogous to Figure 5, we can observe from Figure 6 that the forecasts suggest an increase (decrease) in generated hydropower during above normal (below normal) inflow years. It is important to note that the increase in hydropower generated during the above normal years results from an increased allocation of water for power generation. This also in turn results in a reduced spill from the reservoir during above normal inflow years. The estimated spill each year for both the seasons is shown in Figure 7. We observe that for most of the years the spill obtained from the forecast models is lesser than the spill suggested by the climatological ensemble. This indicates that the model is actually releasing additional water for hydropower generation during above-normal years.

We can always increase the allocation for any use by allocating additional water. But, such an increase should not come at the cost of failing to meet the target storage. To evaluate whether the changes in releases do not result in increased/decreased storage at the end of the season, we show the simulated end of season (June (Figure 8a) and December (Figure 8b)) storages from 1991 -2005 by combining the forecast-suggested releases from both the models with the observed flows. We observe that during below normal years the simulated end of season storage is lesser than the target storage (S_T*). From Figure 8, it is clear that the multimodel forecasts suggested releases keep the storages very close to the target storage in comparison to the storages obtained using the single model forecasts and the climatological ensemble. The only exceptions are during AMJ 2004 and AMJ 2005 where the multimodel forecasts suggest an increased release resulting in a storage that is lesser than the target storage. This is a clear case of multimodel forecasts failing to estimate the target storage. During the rest of the years on both seasons, multimodel forecasts estimate the storages closer to the target storage.

The retrospective reservoir analysis presented in this study can be utilized to determine the appropriate seasonal releases in conjunction with the future streamflow potential. If the forecasts suggest an above normal inflow year, then the $\text{Prob}(S_T < S_T^*)$ will be lower than its climatological probability, forecasts based allocation would facilitate the opportunity to relax the restrictions and thereby release more water for hydropower generation and reduce downstream flood risk. In other words, the reservoir operators can consider additional releases such that the forecasts based estimates of $\text{Prob}(S_T < S_T^*)$ are equal to its climatological probability of p_s=0.5. Similarly, during below normal years, one can consider the options of enforcing restrictions on the releases to ensure the end of season target storage is met with a probability equal to climatological probability. By suggesting a reduction in hydropower generation during below normal inflow years, the system's resilience in rebounding to normal operation is improved by hedging additional water to meet future demand.

Discussion:

Results from the multimodel climate forecasts improve the forecast skill by reducing the overconfidence of individual models (Weigel et al. 2008; Devineni et al. 20010ab). The intent of this study is to utilize them in applying them for improving reservoir management. For this purpose, we considered multimodel precipitation forecasts developed by Devineni et al. (2010b) for developing seasonal inflow forecasts into Masinga Reservoir in the Tana River basin, Kenya. Inflow forecasts developed from multimodel and ECHAM4.5 clearly show that multimodel forecasts have improved skill in predicting the observed flows (Figure 3). Utilizing analyses presented in Figure 4 clearly show that multimodel forecasts reduces the overconfidence of individual model forecasts and also reduces false alarms (e.g., year 1996 in Figure 4a). Except very few instances (OND 1991 in Figure 4b), multimodel forecasts perform better than ECHAM4.5 model-based inflow forecasts in many years (e.g., OND 1995 in Figure 4b) compared to individual model forecasts. It is important to note that for both seasons, AMJ and OND, multimodel forecasts are developed two months (February for AMJ and August for OND) ahead of individual model forecasts, which are issued at the beginning of the season. Another advantage in using multiple models for analyzing the storage probabilities is during normal years. It is very clear from our analysis that the storage probabilities are around a smaller range indicating that a normal or business-as-usual operation could be pursued.

Analyses in Figures 5-7 show that inflow forecasts from climate models could be adjusted to meet the climatological probability of meeting the target storage ($p_s = 0.5$). However, our modeling framework facilitates target-storage probability based on stakeholder’s choice of interest. However, for such selected probabilities, inflow forecasts should be carefully analyzed to ensure the forecasts being well-calibrated indicating a good correspondence between forecast probabilities and their observed relative frequencies (Devineni et al. 2008). Such careful analyses on inflow forecasts based on user-selected target-storage probabilities would reduce apprehensions on utilizing climate-information based streamflow forecasts for improving water and energy management. Our analyses from Figure 8 also show that forecasts-based allocation ensures meeting the target storages in both seasons. Since Figure 8 is obtained by combining forecasts-based releases with the observed inflows, it is a validation of the performance of inflow forecasts in meeting the target storage as well as improving the hydropower generation. The lessons from this study also have potential applications for basins in the Southeast US. This is primarily because both regions (GHA and Southeast) are semi-arid and the river basins are predominantly belonging to rainfall-runoff regime. From hydroclimate perspectives too, Southeast experiences dry and warm winter during La Nino conditions as like the Tana River basin. Our hydroclimatology research group in collaboration with the State Climate Office of NC has developed an online portal (http://www.nc-climate.ncsu.edu/inflowforecast) for disseminating both the inflow forecasts from multiple models and the storage forecasts for the user-specified releases. Our hope is that as multiple climate models are analyzed in developing seasonal forecasts, providing online access to both inflow and storage forecast scenarios will result in real-time evaluation and application of climate-information based streamflow forecasts for improving reservoir operations in regions that are significantly impacted by climate variability.

5.0 Summary and Conclusions

A reservoir simulation model that uses ensembles of streamflow forecasts is presented and applied for improving the water allocation and thereby the energy management for the Masinga Reservoir in Tana River basin in Kenya. The Masinga Reservoir located in the upper Tana River Basin is extremely important in supplying the power requirements of the country as well as in protecting the downstream ecology of the Tana River System. The Dam serves as the primary storage reservoir, controlling streamflow through a series of downstream hydro-electric reservoirs. Prolonged droughts of 1999-2001 in the Tana River basin due to La Nina related conditions resulted in power shortages and prolonged power rationing in Kenya. In this study, we utilize reservoir inflow forecasts downscaled from monthly updated precipitation forecasts from ECHAM4.5 forced with constructed analogue SSTs and multimodel precipitation forecasts developed from ENSEMBLES project to improve the seasonal water allocation during April-June (AMJ) and October-December (OND) seasons for the Masinga reservoir in Kenya. Three-month ahead inflow forecasts developed from ECHAM4.5, multiple General Circulation Models (GCMs) and climatological ensemble are forced into a reservoir simulation model to allocate water for power generation by ensuring climatological probability of meeting the end of the season target storage that is required to meet the water demands during non-rainy seasons. The forecasts based releases are then combined with observed inflows to estimate storages, spill and generated hydropower from the system. Retrospective reservoir analysis shows that inflow forecasts developed from single GCM and multiple GCMs perform better than climatology reduce the spill considerably by increasing the allocation for hydropower during above-normal inflow years. Similarly, during below-normal inflow years, both these forecasts could be effectively utilized to meet the end of the season target storage by restricting the releases of water for power generation uses. Comparing the performance of inflow forecasts developed from multimodels with the inflow forecasts developed using ECHAM4.5 alone, we infer that the multimodel forecasts preserves the end of the season target storage better in comparison to the single model forecasts by reducing the overconfidence of individual model forecasts. Thus, considering multiple models for seasonal water allocation reduces the uncertainty related to a single model and provides the inflow forecasts with reduced model uncertainty for improving water and energy allocation.

Acknowledgements:

We are thankful to NOAA for providing funding for this research through the grant NA09OAR4310146. We also appreciate the comments of three anonymous reviewers which has led to substantial improvements in the manuscript.

References

Balmaseda, M. A., A. Vidard, and D. L. T. Anderson, 2008: The ECMWF ORA-S3 ocean analysis system, Mon. Weather Rev., 136, 3018–3034, doi:10.1175/2008MWR2433.1.

Collins, W. J., et al., 2008: Evaluation of the HadGEM2 model, Tech. Note HCTN 74, Met Off. Hadley Cent., Exeter, U. K.

Daget, N., A. T. Weaver, and M. A. Balmaseda, 2009: Ensemble estimation of background-error variances in a three-dimensional variational data assimilation system for the global ocean, Q. J. R. Meteorol. Soc., 135, 1071–1094, doi:10.1002/qj.412.

Dettinger, M. D., and H. F. Diaz, 2000: Global characteristics of stream flow seasonality and variability. J Hydrometeorol., 1, 289– 310.

Devineni, N. and A. Sankarasubramanian, 2010a: Improved categorical winter precipitation forecasts through multimodel combinations of coupled GCMs. Geophys. Res. Lett., 37, L24704, doi:10.1029/2010GL044989, 1-22.

Devineni, N. and A. Sankarasubramanian, 2010b: Improving the Prediction of Winter Precipitation and Temperature over the Continental United States: Role of ENSO State in Developing Multimodel Combinations. Monthly Weather Review, 138(6), 2447-2468.

Devineni, N., A. Sankarasubramanian, and S. Ghosh, 2008: Multimodel ensembles of streamflow forecasts: Role of predictor state in developing optimal combinations. Water Resour. Res., 44, W09404, doi:10.1029/ 2006WR005855.

Gangopadhyay, S., M. Clark, and B. Rajagopalan, 2005: Statistical downscaling using K-nearest neighbors. Water Resour. Res., 41, W02024, doi:10.1029/2004WR003444.

Georgakakos, K. P., and N. E. Graham, 2008: Potential benefits of seasonal inflow prediction uncertainty for reservoir release decisions. J. Appl. Meteorol. Climatol., 47, 1297–1321, doi:10.1175/2007JAMC1671.1.

Goddard, L., A. G. Barnston, and S. J. Mason, 2003: Evaluation of the IRI's ‘‘net assessment’’ seasonal climate forecasts: 1997–2001. Bull. Am. Meteorol. Soc., 84, 1761– 1781, doi:10.1175/BAMS-84-12-1761.

Golembesky, K., A. Sankarasubramanian, and N. Devineni, 2009: Improved drought management of Falls Lake Reservoir: Role of multimodel streamflow forecasts in setting up restrictions. J. Water Resour. Plann. Manage., 135(3), 188–197, doi:10.1061/(ASCE)0733-9496(2009)135:3(188).

Hamlet, A. F., and D. P. Lettenmaier, 1999: Columbia River streamflow forecasting based on ENSO and PDO climate signals. *J. Water Resour. Plann. Manage.*, 125(6), 333–341.

Keenlyside, N. S., M. Latif, M. Botzet, J. Jungclaus, and U. Schulzweida, 2005: A coupled method for initializing El Niño Southern Oscillation forecasts using sea surface temperature, Tellus, Ser. A, 57, 340–356.

Kyriakidis, P. C., N. L. Miller, and J. Kim, 2001: Uncertainty propagation of regional climate model precipitation forecasts to hydrologic impact assessment. *J Hydrometeorol.*, 2, 140–160.

Leung, L. R., A. F. Hamlet, D. P. Lettenmaier, and A. Kumar, 1999: Simulations of the ENSO hydroclimate signals in the Pacific Northwest Columbia River basin. Bull. Am. Meteorol. Soc., 80(11), 2313–2329, doi:10.1175/1520-0477(1999)080<2313:SOTEHS>2.0.CO;2.

Li, S. and L. Goddard, 2005: Retrospective Forecasts with the ECHAM4.5 AGCM, IRI Technical Report, 05–02, available at: http://iri.columbia.edu/outreach/publication/report/05-02/report05-02.pdf, The Earth Institue, Columbia University, New York.

Maurer, E. P. and D. P. Lettenmaier, 2003: Predictability of seasonal runoff in the Mississippi River basin. J. Geophys. Res., 108(D16), 8607, doi:10.1029/2002JD002555.

Mogaka, H., S. Gichere, R. Davis, and R. Hirji, 2006: Climate Variability and Water Resources Degradation in Kenya Improving Water Resources Development and Management, THE WORLD BANK, working paper no. 69, Washington, D.C., 130pp, http://www-wds.worldbank.org/servlet/WDSContentServer/WDSP/IB/2006/01/10/000090341_20060110161654/Rendered/PDF/348540KE0Clima101OFFICIAL0USE0ONLY1.pdf

Mutai, C.C. and M.N. Ward, 2000: East African rainfall and the tropical circulation/convection on intraseasonal to interannual timescales, Journal of Climate 13 (22), 3915-3939.

Nijssen, B., G. M. O’Donnel, A. F. Hamlet, and D. P. Lettenmaier, 2001: Hydrologic sensitivity of global rivers to climate change. Clim. Change, 50, 143–175, doi:10.1023/A:1010616428763.

Oludhe, C., S.Marigi, and D.Kimani (2004), An assessment of the potential benefits of seasonal rainfall prediction in relation to hydroelectric power generation, Pilot application project report, Drought Monitoring Center, Nairobi.

Pagano, T. C., H. C. Hartmann, and S. Sorooshian, 2002: Factors affecting seasonal forecast use in Arizona water management: A case study of the 1997– 98 El Nin˜o. Clim. Res., 21(3), 259– 269, doi:10.3354/cr021259.

Pagano, T. C., H. C. Hartmann, and S. Sorooshian, 2001: Using climate forecasts for water management: Arizona and the 1997–1998 El Nino. *J. Am. Water Resour. Assoc.*, 37(5), 1139–1153.

Piechota, T. C., and J. A. Dracup, 1996: Drought and regional hydrologic variation in the United States: Associations with the El Nin˜o – Southern Oscillation. Water Resour. Res., 32, 1359 – 1374, doi:10.1029/ 96WR00353.

Piechota, T. C., F. H. S. Chiew, J. A. Dracup, and T. A. McMahon, 2001: Development of exceedance probability streamflow forecast. J. Hydrol. Eng., 6(1), 20–28, doi:10.1061/(ASCE)1084-0699(2001)6:1(20).

Rajagopalan, B., U. Lall, and S. E. Zebiak, 2002: Categorical climate forecasts through regularization and optimal combination of multiple GCM ensembles. Mon. Wea. Rev., 130, 1792–1811.

Robertson, A. W., S. Kirshner, and P. Smyth, 2004: Downscaling of daily rainfall occurrence over northeast Brazil using a hidden Markov model. J. Climate, 17, 4407–4424.

Ropelewski, C. F., and M. S. Halpert, 1987: Global and regional scale precipitation patterns associated with the El-Nino southern oscillation. *Mon. Weather Rev.*, 115(8), 1606-1626.

Sankarasubramanian, A., U. Lall, and S. Espinueva, 2008: Role of retrospective forecasts of GCMs forced with persisted SST anomalies in operational streamflow forecasts development. J. Hydrometeorol., 9, 212– 227, doi:10.1175/2007JHM842.1.

Sankarasubramanian, A., U. Lall, N. Devineni, and S. Espinueva, 2009: The role of monthly updated climate forecasts in improving intraseasonal water allocation. J. Appl. Meteorol. Climatol., 48, 1464– 1482.

Sicard, E., R. Sabatier, H. Niel, and E. Cadier, 2002: A new approach in space-time analysis of multivariate hydrological data: Application to Brazil's nordeste region rainfall. Water Resour. Res., 38(12), 1319, doi:10.1029/2002WR001413.

Souza Filho, F. A., and U. Lall, 2003: Seasonal to interannual ensemble streamflow forecasts for Ceara, Brazil: Applications of a multivariate, semiparametric algorithm. Water Resour. Res., 39(11), 1307, doi:10.1029/2002WR001373.

Voisin, N., A. F. Hamlet, L. P. Graham, D.W. Pierce, T. P. Barnett, and D. P. Lettenmaier, 2006: The role of climate forecasts in western US power planning. J. Appl. Meteorol. Climatol., 45, 653–673, doi:10.1175/ JAM2361.1.

Weigel, A. P., M. A. Liniger, and C. Appenzeller, 2008: Can multi-model combination really enhance the prediction skill of probabilistic ensemble forecasts? Quart. J. Roy. Meteor. Soc., 134, 241–260.

Weisheimer, A., and Coauthors, 2009: ENSEMBLES: A new multimodel ensemble for seasonal-to-annual predictions—Skill and progress beyondDEMETERin forecasting tropical Pacific SSTs.Geophys. Res. Lett., 36, L21711, doi:10.1029/2009GL040896.

Wilks, D. S., 1995: Statistical Methods in the Atmospheric Sciences: An Introduction, Academic Press, 467 pp.

List of Figures

Figure 1: (a) Location of the Upper Tana River Basin in Kenya with letters representing the following dams: A – Kiambere, B – Kindaruma, C – Gitaru, D – Kamburu, and E - Masinga, and (b) Seasonal variation of the AMJ and OND total inflows into Masinga Dam (1947 – 2005).

Figure 2: Comparison between the observed and predicted inflows into Masinga Dam using Single (SM) and Multimodel (MM) for (a): AMJ and (b) OND seasons.

Figure 3: (a) Masinga Operational Rule Curves, and (b) Comparison between observed (Obs) and simulated (Sim) June end storage.

Figure 4: Comparison between climatology and inflow-forecast based estimates of failure probabilities in meeting (a) June (Jun) end storage and (b) December (Dec) end storage for single model (SM) and Multimodel (MM). Empty circles denote observed inflows during normal years (Obs), gray filled circles show inflows during below normal years (Obs_BN, less than 33^{rd} percentile), and black filled circles show inflows during above normal years (Obs_AN, greater than 67^{th} percentile).

Figure 5: Estimated differences in releases suggested by the climatological ensembles to the releases obtained based on single model (SM) and multimodel (MM) forecasts for improving the hydropower generation at Masinga Dam during the (a) AMJ and (b) OND seasons. Empty circles denote observed inflows during normal years (Obs), gray filled circles show inflows during below normal years (Obs_BN, less than 33^{rd} percentile), and black filled circles show inflows during above normal years (Obs_AN, greater than 67^{th} percentile).

Figure 6: Estimated change in electrical power generation at Masinga Dam during the (a) AMJ and (b) OND season using Single Model (SM) and Multimodel (MM). Empty circles denote observed inflows during normal years (Obs), gray filled circles show inflows during below

normal years (Obs_BN, less than 33rd percentile), and black filled circles show inflows during above normal years (Obs_AN, greater than 67th percentile).

Figure 7: Comparison between the observed and predicted spill for the (a) AMJ and (b) OND seasons Dam using Single Model (SM) and Multimodel (MM).

Figure 8: Comparison between the (a) June end and (b) December end storage for Single Model (SM) and Multimodel (MM). Empty circles denote observed inflows during normal years (Obs), gray filled circles show inflows during below normal years (Obs_BN, less than 33rd percentile), and black filled circles show inflows during above normal years (Obs_AN, greater than 67th percentile).

738 **Table 1**: Details of CGCMs considered from the ENSEMBLES project for developing
739 multimodel forecasts for this study.
740

Ocean Model	Atmospheric Model	Institution	Reference
HOPE	IFS CY31R1	ECMWF	Balmaseda et al. (2008)
HadGEM2-O	HadGEM2-A	UKMO	Collins et al. (2008)
OPA8.2	ARPEGE4.6	MF	Daget et al. (2009)
MPI-OMI	ECHAM5	IFM-GEOMAR	Keenlyside et al. (2005)
OPA8.2	ECHAM5	CMCC-INGV	Weisheimer et al. (2009)

741

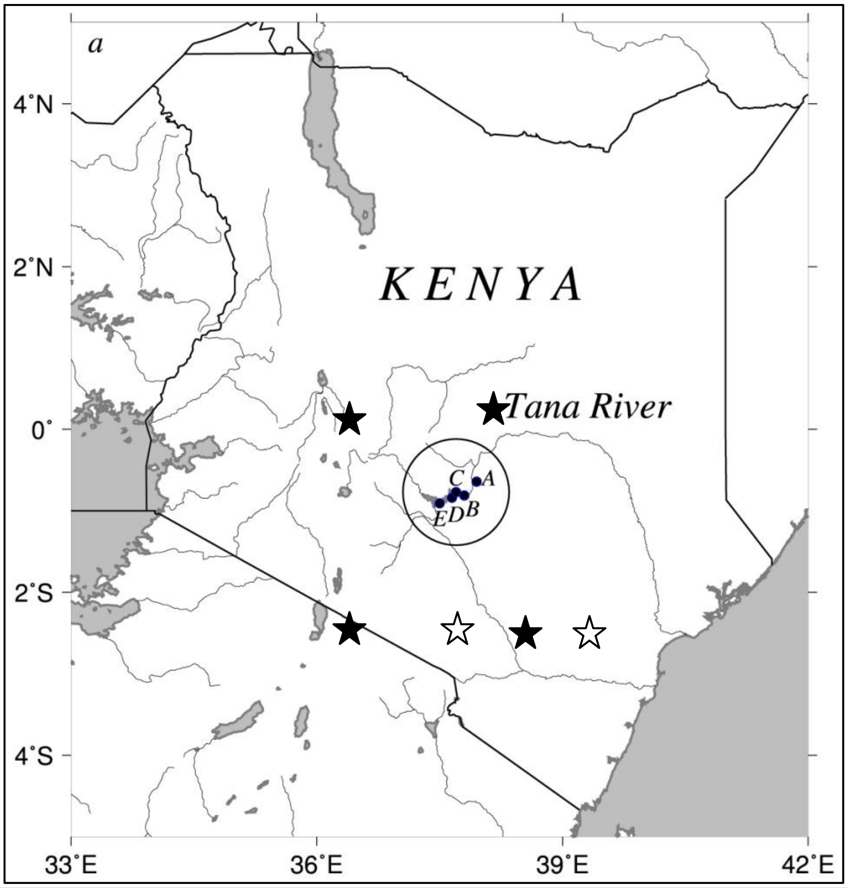

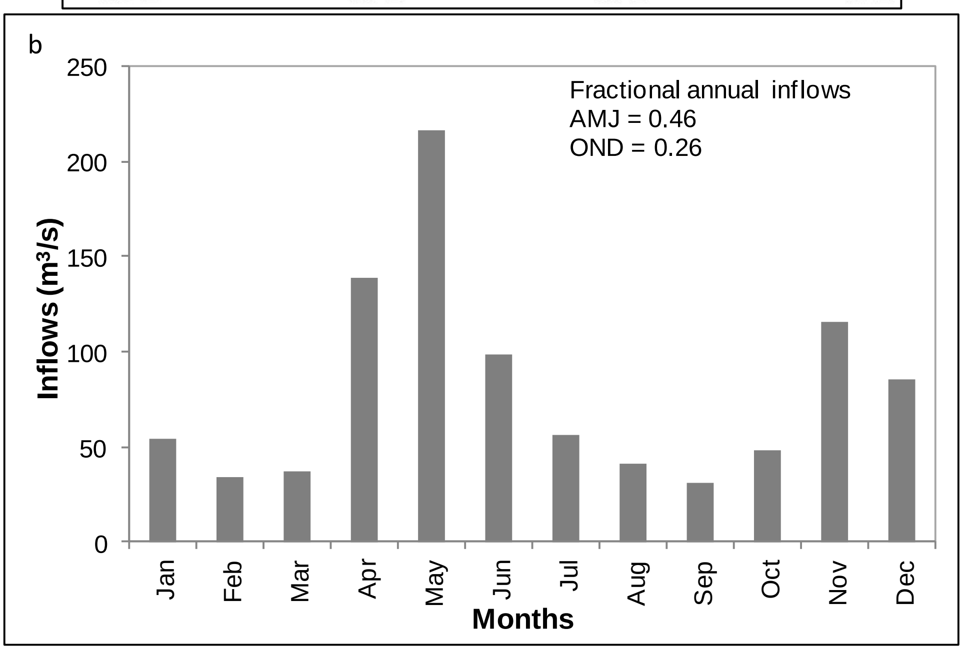

Figure 1: (a) Location of the Upper Tana River Basin in Kenya with letters representing the following dams: A – Kiambere, B – Kindaruma, C – Gitaru, D – Kamburu, and E - Masinga, and (b) Seasonal variation of the AMJ and OND total inflows into Masinga Dam (1947 – 2005). Filled stars in Figure 1a indicate the selected grid points of multimodel forecasts and open stars indicate the selected grid points of ECHAM4.5 GCM.

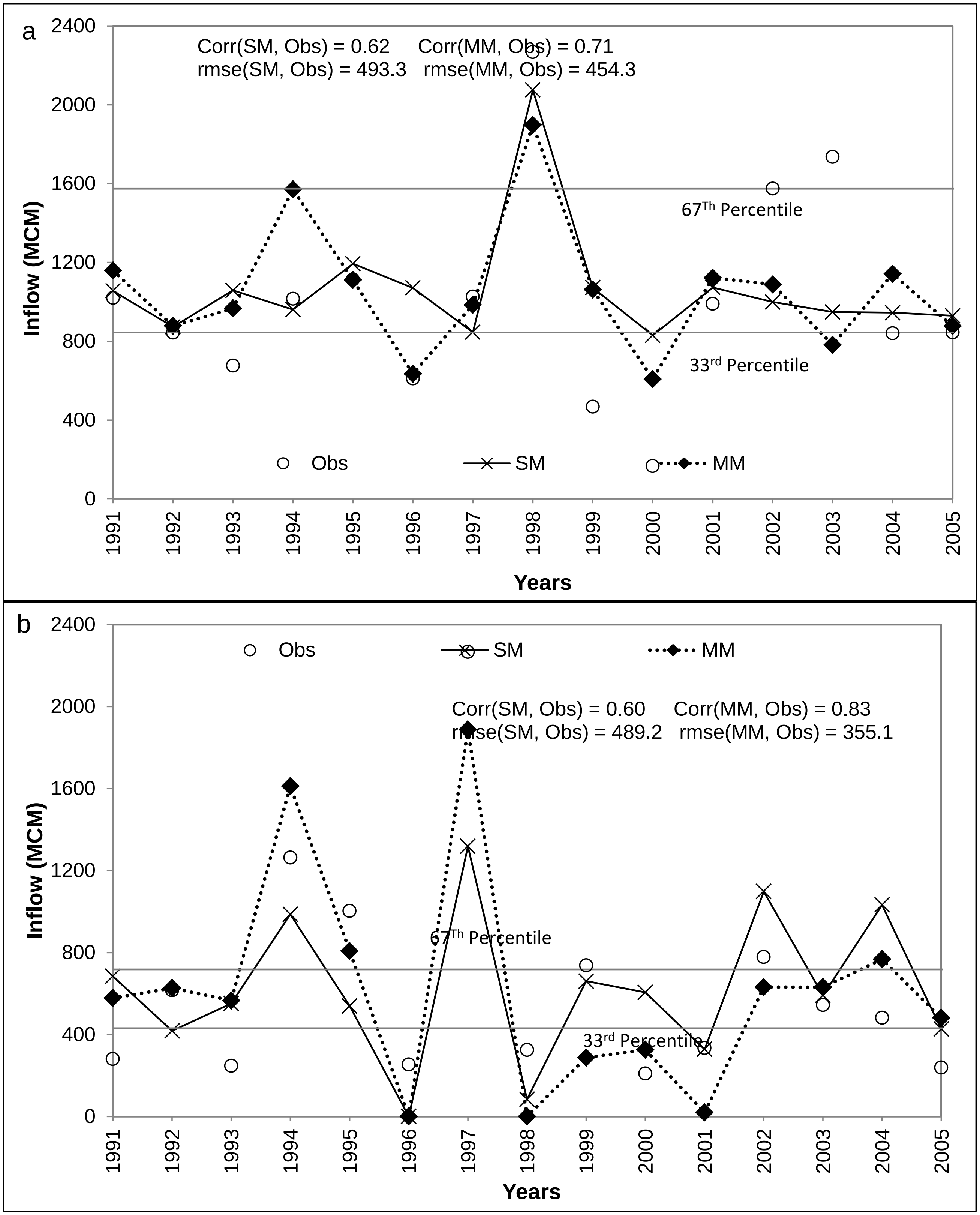

Figure 2: Comparison between the observed and predicted inflows into Masinga Dam using Single (SM) and Multimodel (MM) for (a): AMJ and (b) OND seasons.

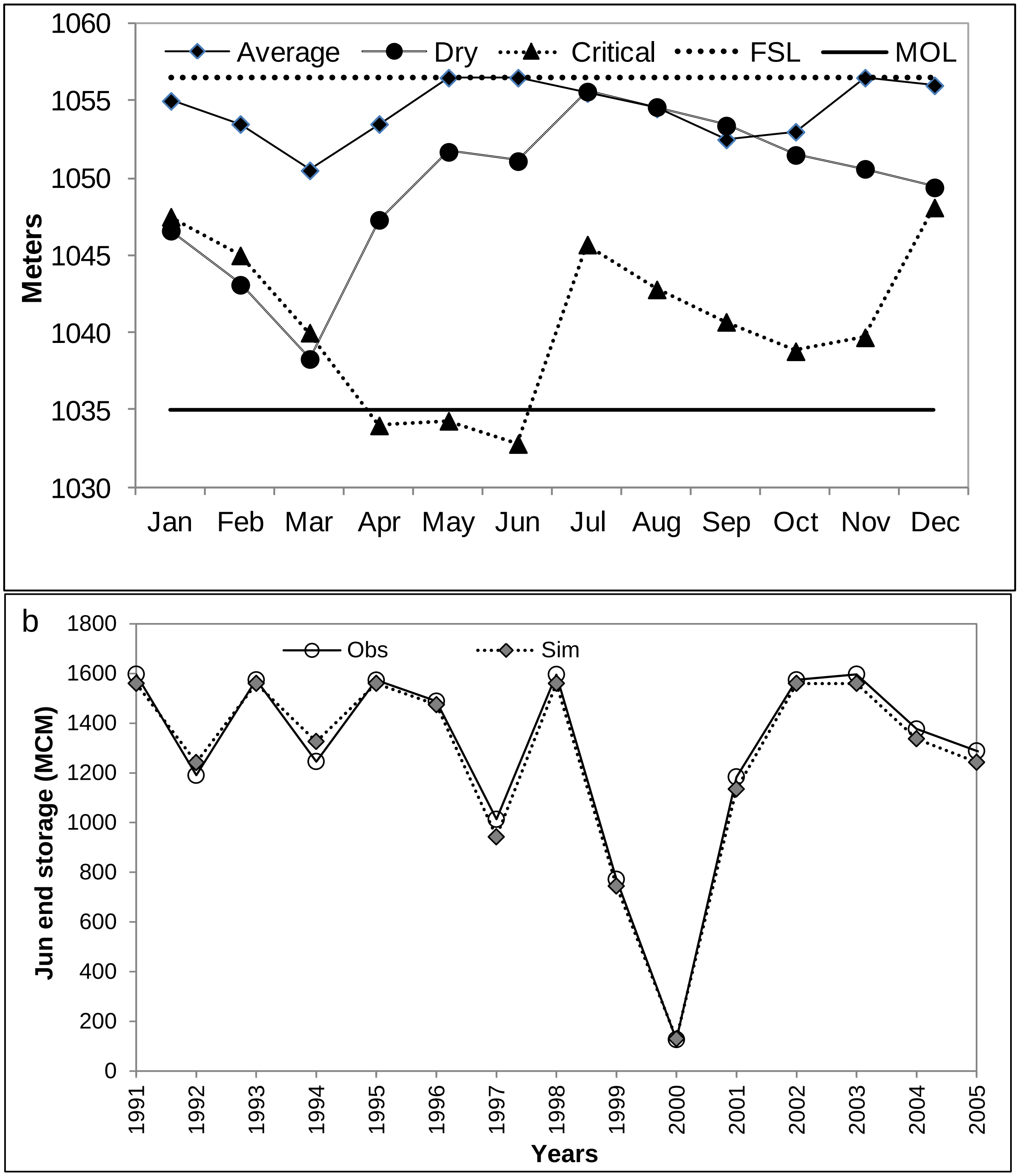

Figure 3: (a) Masinga Operational Rule Curves, and (b) Comparison between observed (Obs) and simulated (Sim) June end storage

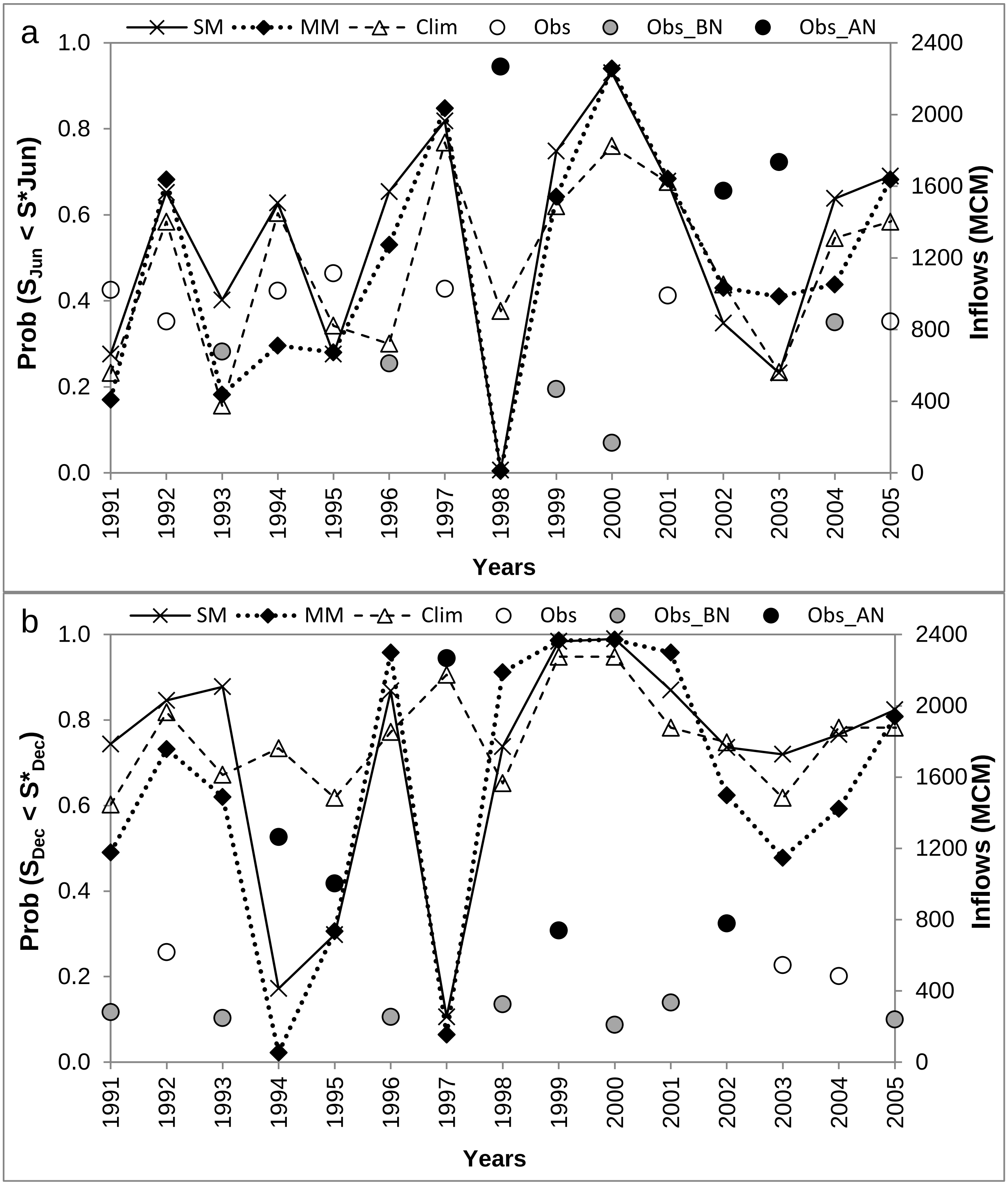

Figure 4: Comparison between climatology and forecast estimates of failure probabilities in meeting (a) June (Jun) end storage and (b) December (Dec) end storage for single model (SM) and Multimodel (MM). Empty circles denote observed inflows during normal years (Obs), gray filled circles show inflows during below normal years (Obs_BN, less than 33rd percentile), and black filled circles show inflows during above normal years (Obs_AN, greater than 67th percentile)

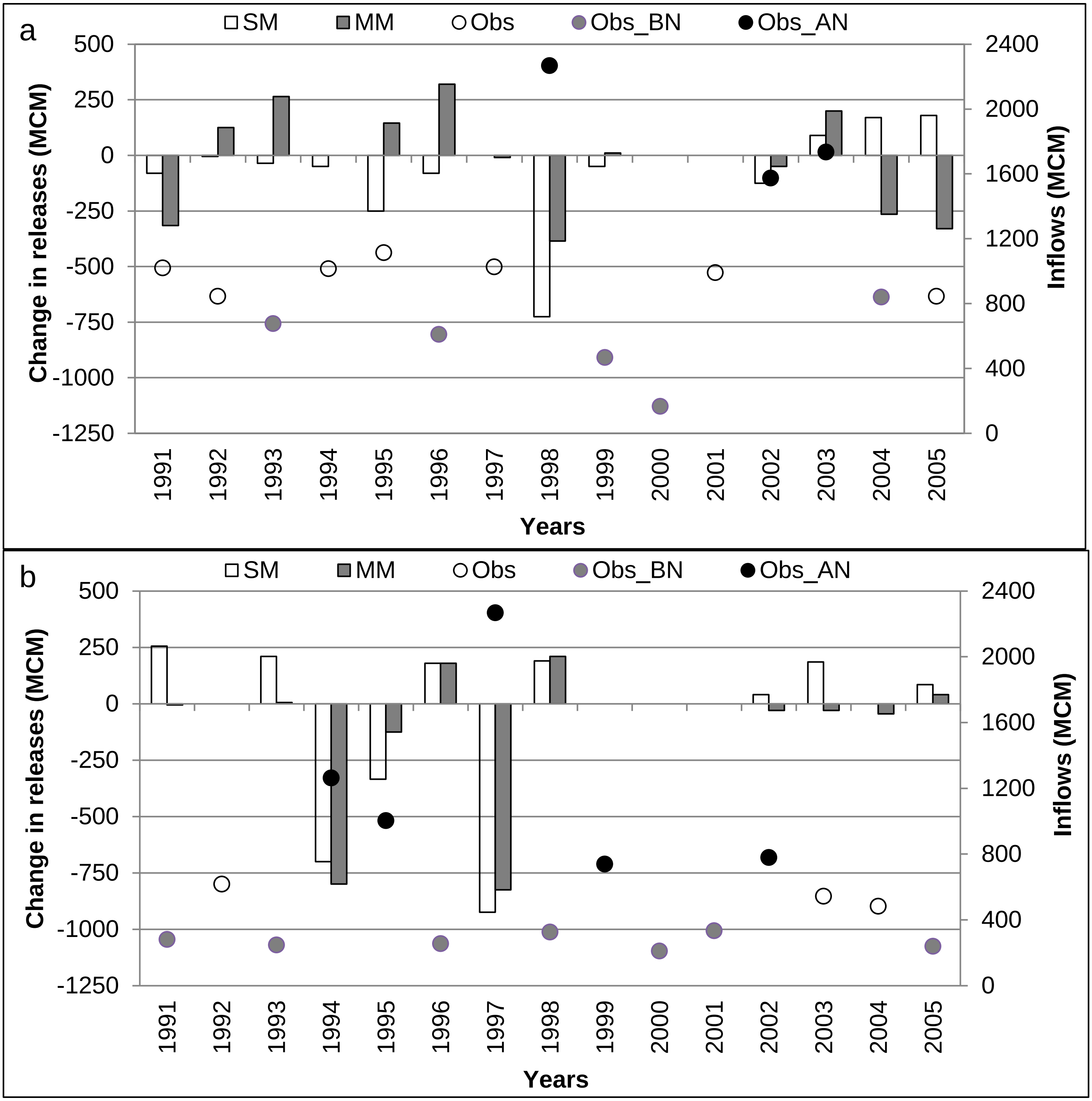

Figure 5: Estimated changes in water releases for power generation at Masinga Dam during the (a) AMJ and (b) OND seasons using single model (SM) and multimodel (MM). Empty circles denote observed inflows during normal years (Obs), gray filled circles show inflows during below normal years (Obs_BN, less than 33rd percentile), and black filled circles show inflows during above normal years (Obs_AN, greater than 67th percentile)

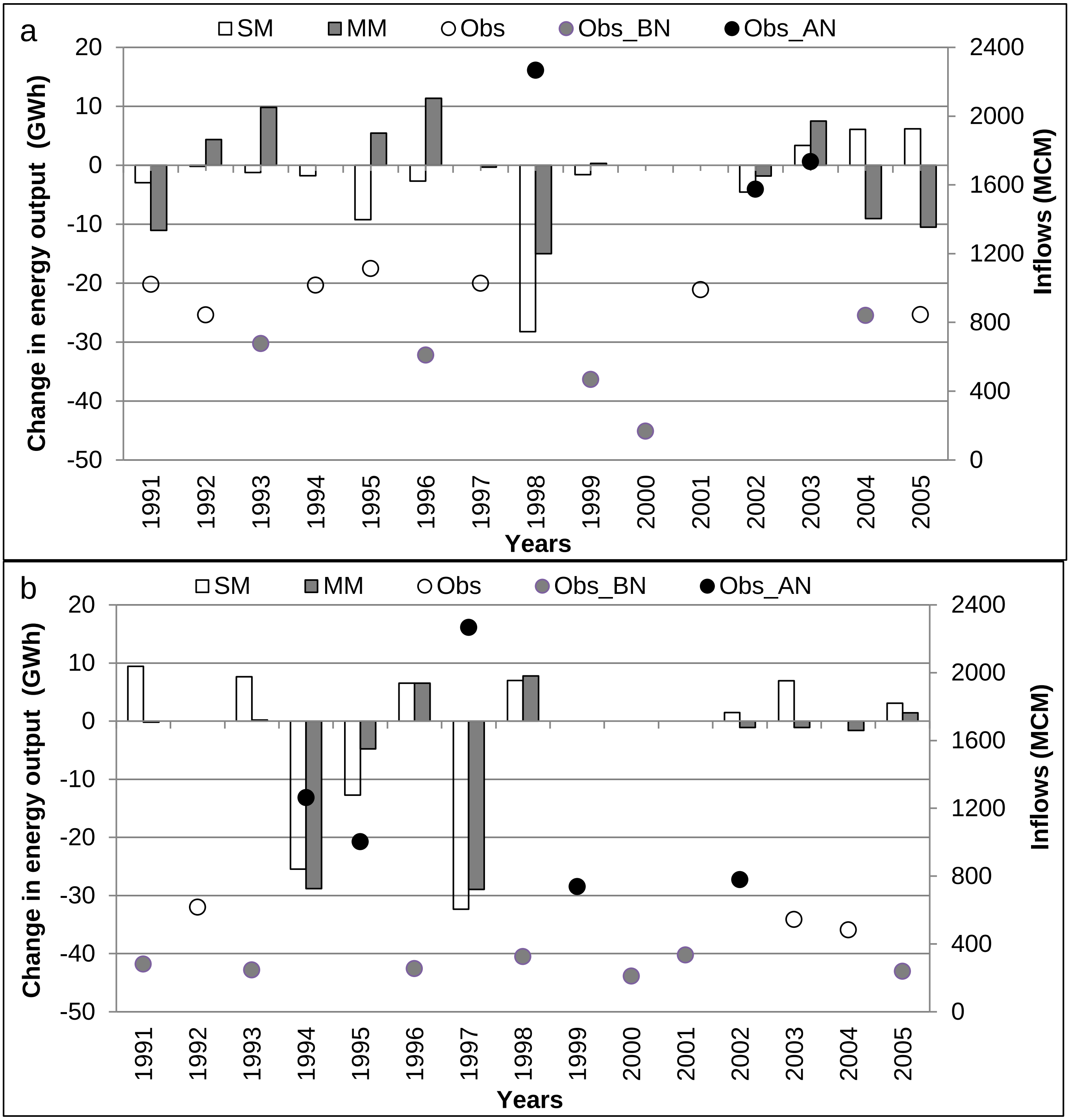

Figure 6: Estimated change in electrical power generation at Masinga Dam during the (a) AMJ and (b) OND season using Single Model (SM) and Multimodel (MM). Empty circles denote observed inflows during normal years (Obs), gray filled circles show inflows during below normal years (Obs_BN, less than 33rd percentile), and black filled circles show inflows during above normal years (Obs_AN, greater than 67th percentile)

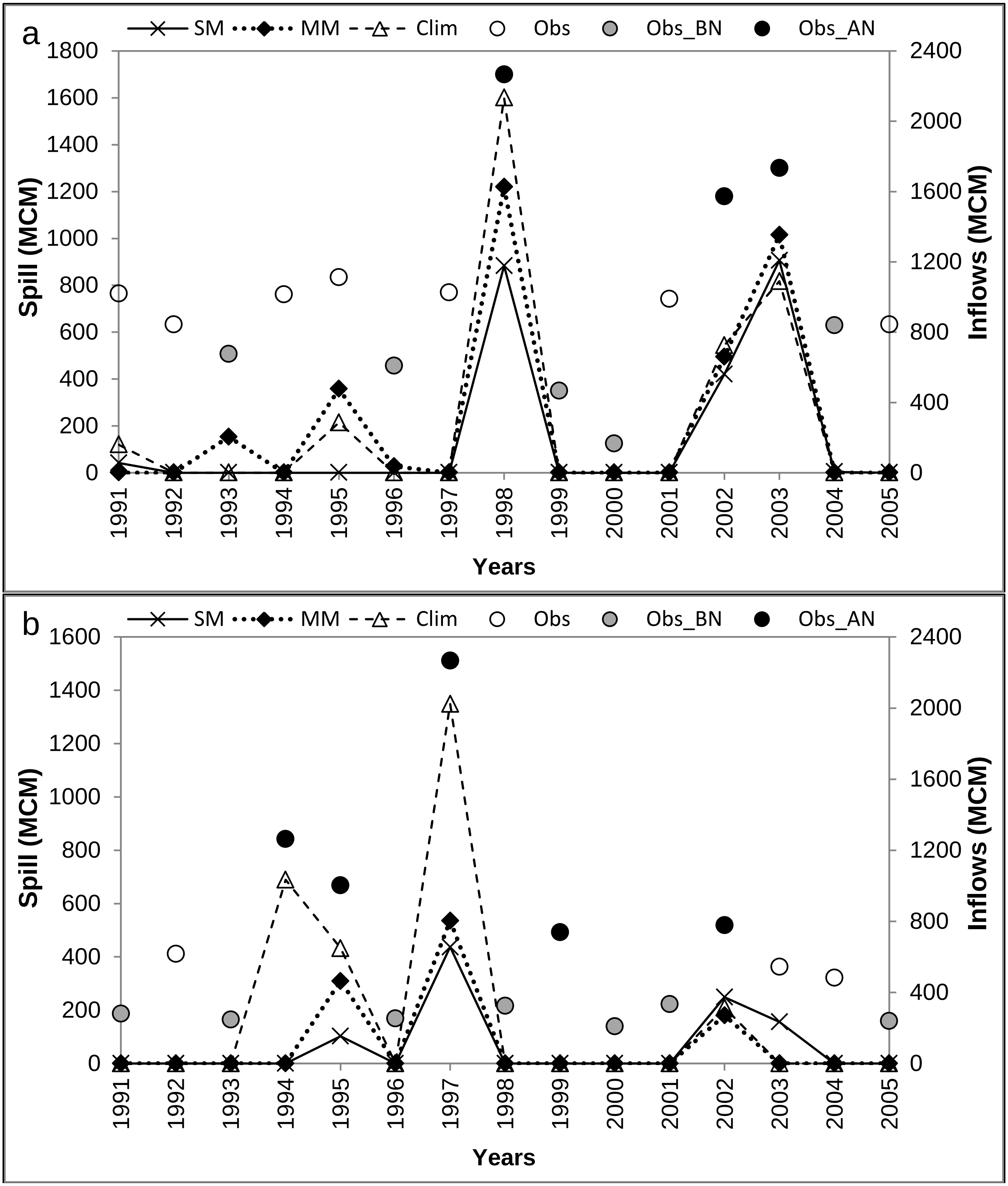

Figure 7: Comparison between the observed and predicted spill for (a) AMJ and (b) OND seasons using Single Model (SM) and Multimodel (MM).

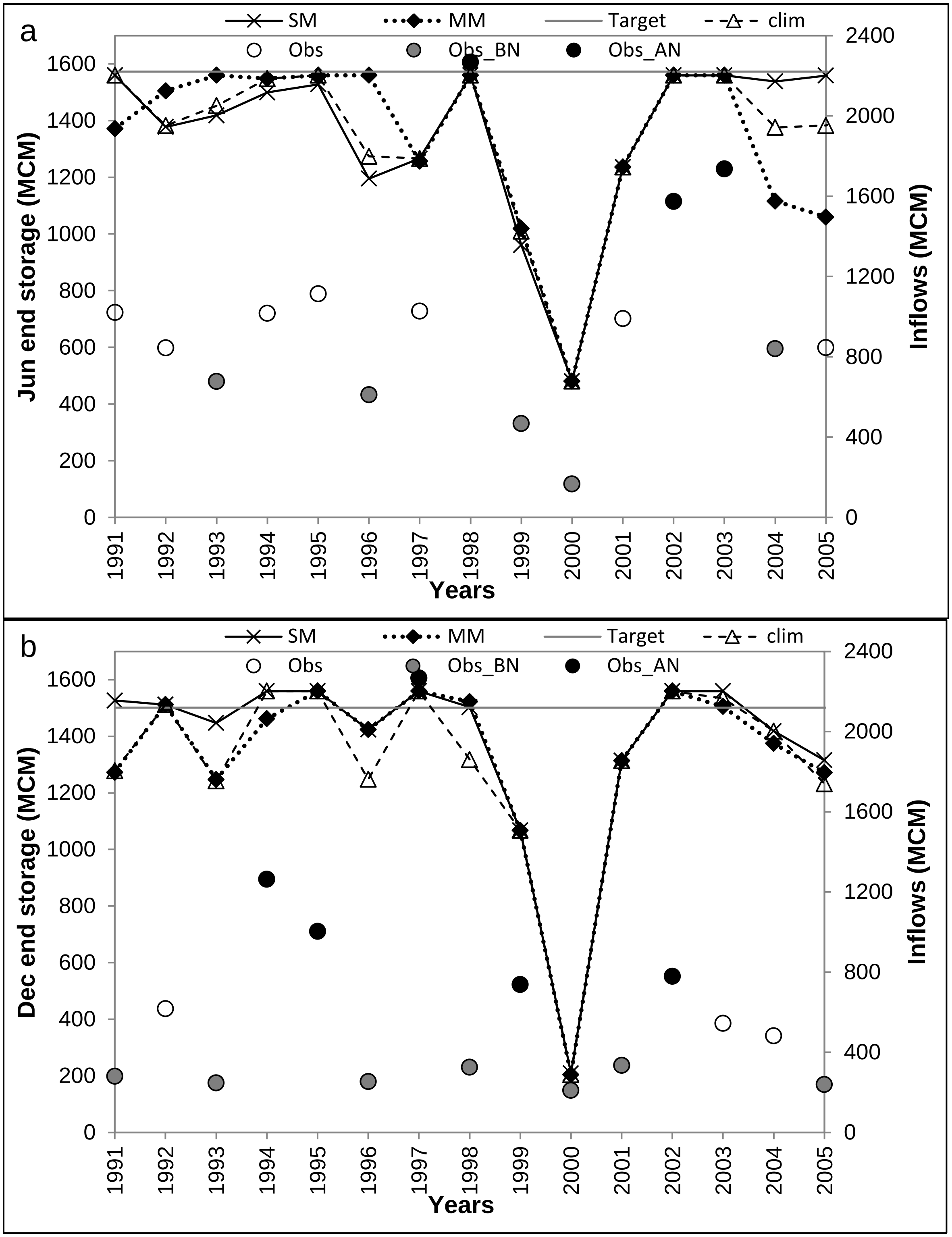

Figure 8: Comparison between the (a) June end and (b) December end storage for Single Model (SM) and Multimodel (MM). Empty circles denote observed inflows during normal years (Obs), gray filled circles show inflows during below normal years (Obs_BN, less than 33rd percentile), and black filled circles show inflows during above normal years (Obs_AN, greater than 67th percentile).